

Hierarchical mesophases of vortex matter in layered superconductors

Christopher N. Varney,¹ Karl A. H. Sellin,² Qingze Wang,^{1,3} Hans Fangohr,⁴ and Egor Babaev^{1,2}

¹*Department of Physics, University of Massachusetts, Amherst, Massachusetts 01003, USA*

²*Department of Theoretical Physics, The Royal Institute of Technology, SE-10691 Stockholm, Sweden*

³*Department of Physics, The Pennsylvania State University, University Park, Pennsylvania 16802, USA*

⁴*Engineering and the Environment, University of Southampton, United Kingdom*

We demonstrate the possible formation of hierarchical mesophases of vortex matter in layered superconducting systems where there are variations of interlayer thicknesses and layers are made of different superconducting materials. We show that because inter-vortex forces feature multiple length scales in this case the magnetic response features the formation of mesophases such as clusters of vortex clusters, concentric vortex rings, vortex clusters in a ring, and vortex stripes in a cluster.

PACS numbers: 74.25.Uv, 74.25.Dw, 74.45.+c

Condensed matter physics has long been concerned with explaining phenomena that result from competing interactions, covering a wide variety of topics from soft condensed matter systems to magnetism and ultracold atoms (for a recent overview see e.g. [1, 2]). The richest pattern forming systems are those with several length scales. For example, structure formation in systems with two-scale repulsive interactions is highly relevant in hard condensed matter systems [3, 4], nuclear matter [5], and in colloids and other soft condensed matter systems [6, 7].

By contrast research on the magnetic response of type-2 superconductors traditionally deals with structure formation of vortices [8]. Although the interaction between vortices in these materials has a simple monotonically repulsive form, the vortex matter exhibits a plethora of interesting phase transitions and structure formation [9]. Moreover, the vortex states, especially in the presence of pinning, are critically important for technological applications of superconductors, where control over vortex matter in many cases amounts to control of dissipation.

Recently, the possibility of more complicated inter-vortex interactions in newly discovered systems has attracted much attention in various contexts: in multi-component superconductors [1, 10–26], superfluids [27], vortices in dense nuclear matter in neutron stars [28], and quantum Hall systems [4]. Recently a problem which attracted interest was the phase separation in vortex matter with long-range attractive and short-range repulsive inter-vortex interactions. Such forces in multi-component superconductors originate in the regime where there are several superconducting components originating from different bands. This gives rise to two coherence lengths, ξ_1 and ξ_2 , and the magnetic field penetration length falls between them: $\xi_1 < \lambda < \xi_2$ [10]. This phenomena, recently referred to as “type-1.5 superconductivity” [11], is the subject of a recent review [29] and has stoked considerable experimental interest in pursuing a realization of such regimes using artificial structures made of alternating layers of type-1 and type-2 materials.

Here we propose that superconducting systems can have vortex states with several length scales of repul-

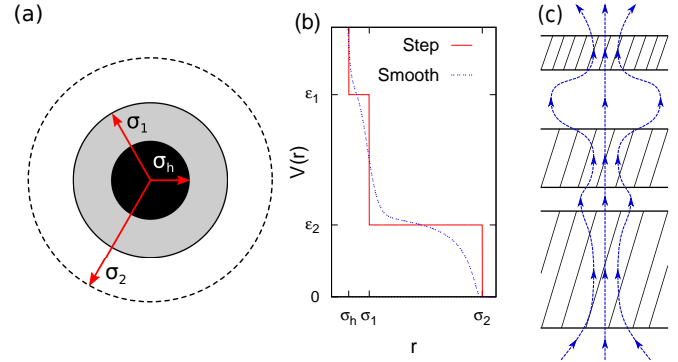


FIG. 1: (Color online) (a) Sketch of a vortex showing interaction length scales. σ_h is the hard-core radius and σ_1 (σ_2) is the inner (outer) soft-core radius. (b) Pair potential $V(r)$ as a function of the interparticle separation r for a step potential and an analogous smooth potential. (c) Schematic drawing of the field lines of a vortex in a layered superconductor. Shaded (white) regions are superconducting (insulation) of varying thickness. By controlling thickness of the of insulating layers one can control intervortex interaction. Thicker insulating layers cause a wider spread of the magnetic field lines resulting in the presence of an additional repulsive length in the intervortex interaction scales.

sive (also in some cases attractive) interactions, where more complicated interaction potentials can be realized. Such intervortex forces should arise in layered structures made of combinations of type-2 and type-1 superconductors where the magnetic field penetration length varies in different layers or where there are insulating layers of varying thickness. Also, for quasi-two-dimensional systems an additional repulsive interaction is present due to the interaction of stray fields outside the sample [30]. Here we consider the regime where vortex line tension is large and temperature is small so the vortices do not bend and we have effective two-dimensional system where vortices can be described by their positions in xy -plane.

With this physical realization in mind, let us consider the simplest potential with several length scales, a hard sphere model with multiple shoulders. Note that

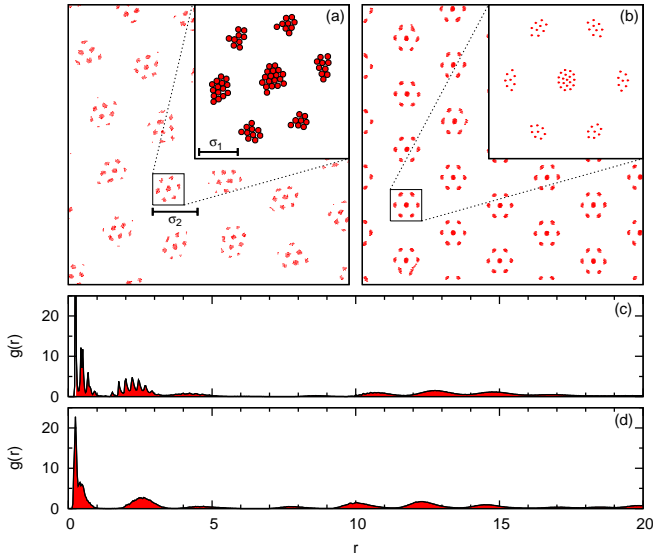


FIG. 2: (Color online) Final particle configuration for (a) three-step potential of Fig. 1(b) and (b) smoothed potential with $N_v = 2000$ and $\rho = 0.51$. The corresponding radial distribution functions are plotted versus particle separation (in units of the characteristic simulation length λ [34]) in panels (c) and (d), respectively.

“core-softened” potentials with a single shoulder have been studied intensively, revealing a myriad of density-modulated ground states [6, 7, 31–33]. In Figs. 1(a) and 1(b) we illustrate a particle with an impenetrable hard-core radius σ_h and two repulsive shoulders at $r = \sigma_1$ and σ_2 with heights ε_1 and ε_2 , respectively.

We show the final configuration from Monte Carlo (MC) simulations [34, 35] of our hard-sphere model in Fig. 2(a) for $N_v = 2000$ particles and density $\rho = 0.51$. Here the system forms a mesophase: namely the particles order on three different length scales: (1) the particles form a tightly bound cluster, (2) the clusters are themselves bound into a conglomerate structure (hereafter referred to as a supercluster), and (3) the structures form a lattice. To analyze the underlying structure of this phase, we show the radial distribution function (RDF) $g(r)$ [34, 36] in Fig. 2(c). The first feature in $g(r)$ is a very strong peak corresponding to the nearest-neighbor distance inside each cluster. Because the clusters have such a small radius, $g(r)$ shows only a small peak at approximately double the nearest-neighbor distance. The next pronounced peak is the inter-cluster distance inside a supercluster, with the subsequent peaks describing the distance between clusters in different superclusters.

A more physically accurate potential is achieved by smoothing out the steps in the previous potential [see Fig. 1(b)]. In Fig. 2(b), we show the final MC configuration for the smooth potential, which is a supercluster of higher radial symmetry. The RDF is plotted in Fig. 2(d) and has nearly identical features, although the

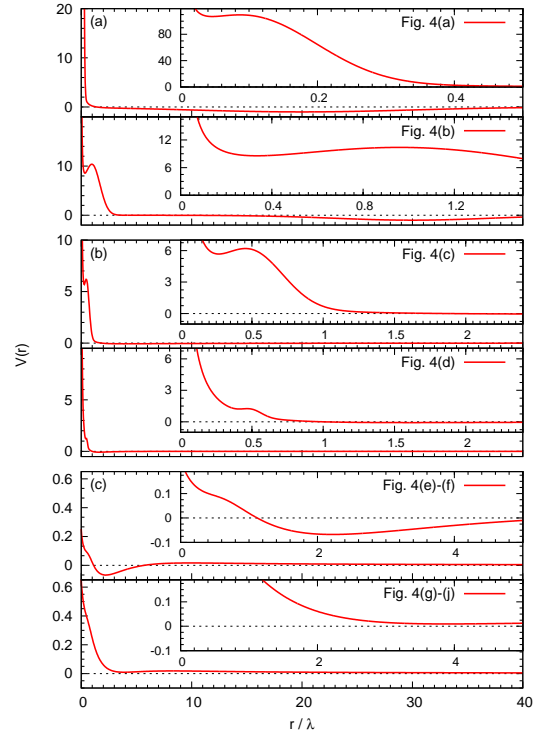


FIG. 3: (Color online) Inter-vortex pair potentials used in this study. Panels (a), (b), and (c) each illustrate a different pair potential, with the top and bottom of each panel representing a different set of parameters [34]. The insets are close up views of the potentials for small interparticle separation. The legend indicates the corresponding panels in Fig. 4.

higher symmetry of the ground state results in smoother peaks. The conclusions that follow are (i) multiple repulsive length scales result in a formation of hierarchical structures and (ii) the precise form of the potential is of a lesser importance in this example: the crucial aspect is the existence of several length scales in the interaction.

To classify possible mesophases we need to consider what sorts of vortex structures exist in systems where there exist competing interactions that are dominant at different length scales (see Fig. 3). In the context of Fig. 1, such systems can be realized by adding layers of type-1 material or alternating layers of clean and dirty material, while repulsive scales are tunable by controlling e.g. layer thicknesses.

In Fig. 3(a), we show two potentials that both feature a strong repulsive core surrounded by an area of attraction. Outside the attractive shell, there is a repulsive region and an attractive long-range coupling. At very low vortex densities, the final MC configurations for both of these potentials are given in Fig. 4(a) and Fig. 4(b), respectively. In the first case, the particles form a cluster due to their attractive interaction, the repulsive scale however gives this cluster a ring shape. In the second, the combination of attractive and repulsive scales induces

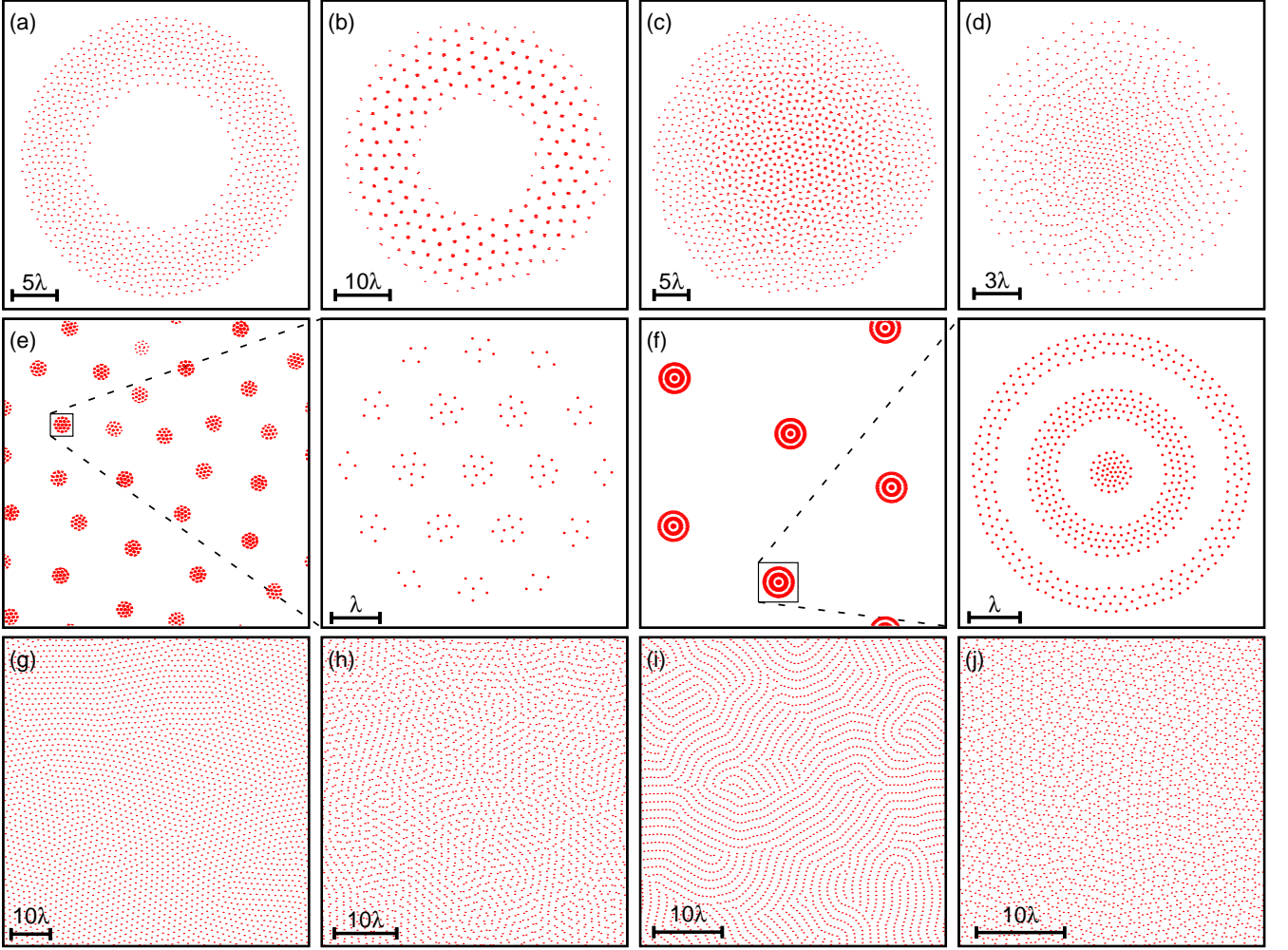


FIG. 4: (Color online) Snapshot of the final vortex configurations corresponding to the potentials in (a) top panel of Fig. 3(a) with $N_v = 1000$ and density $\rho = 0.044$, (b) bottom panel of Fig. 3(a) with $N_v = 1000$ and density $\rho = 0.025$, (c) top panel of Fig. 3(b) with $N_v = 2000$ and $\rho = 0.20$, (d) bottom panel of Fig. 3(b) with $N_v = 1000$ and $\rho = 0.40$, top panel of Fig. 3(c) with $N_v = 3000$ and densities (e) $\rho = 0.25$ and (f) $\rho = 1.00$, and the bottom panel of Fig. 3(c) with $N_v = 3000$ and densities (g) $\rho = 0.50$, (h) $\rho = 1.25$, (i) $\rho = 1.50$, and (j) $\rho = 2.50$. For panels (a), (b), (c), and (d), the long-range attraction causes all of the particles to form a single object and we only show a close up view. The unlabeled panels are close-up views of panels (e) and (f), focusing on a single supercluster and ring, respectively. The final vortex configurations in panels (a)-(d) and panels (e-j) are from Monte Carlo [35] and Molecular Dynamics [37] simulations, respectively, with simulation details discussed in Ref. 34.

clustering inside the ring (a clustered ring).

Next, we consider two potentials where the long-range attraction is extremely weak and we vary the potential at intermediate length scales [see Fig. 3(b)]. The final MC configurations for these potentials at densities $\rho = 0.2$ and $\rho = 0.8$ are shown in Figs. 4(c) and 4(d). In the first case, the particles form a single large supercluster with one critical difference from the case shown on Fig. 2: the size of the constituent small clusters is modulated by the distance to the center of the cluster, going from a maximum of 4 vortices per cluster in the center to a shell of single vortices at the edge. In the second case, when the interaction in the intermediate region is modified, the local phase of the cluster varies with distance from the cen-

ter: namely as one goes from the center of the cluster to the edge one encounters regions corresponding to vortex lattice, vortex stripes, and vortex voids phases. Here the long range attractive interaction makes the vortex density gradually increase towards the center of the cluster leading to a sequence of mesophases which optimize the interaction associated with repulsive short-range scales.

The third pair of potentials [see Fig. 3(c)] we examine feature a moderate repulsive core surrounded by an attractive well and have a long-range repulsive interaction. When the well is strong, the final vortex configurations from Molecular Dynamics (MD) simulations [34, 37, 38] are circular superclusters at a density $\rho = 0.25$ or concentric rings at a density of $\rho = 1$ [illustrated in Figs. 4(e)

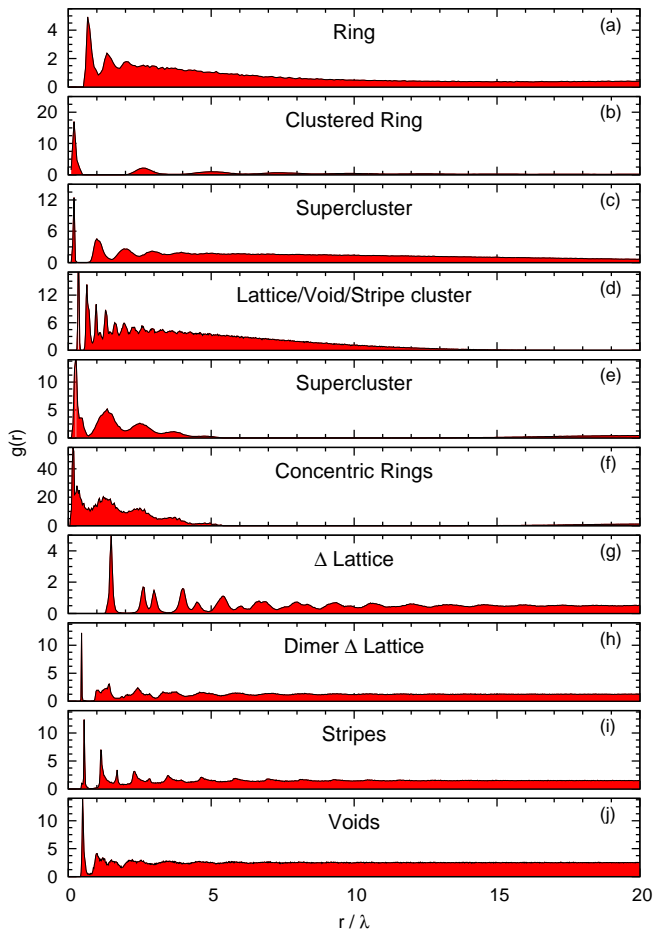


FIG. 5: (Color online) Radial distribution function $g(r)$ corresponding to the phases illustrated in Fig. 4.

and 4(f)]. Again the short-range structure is determined by repulsive length scales. However, when the attractive well is weakened significantly more regular repulsion-dominated vortex phases appear at higher densities [see Figs. 4(g)-(j)]: a triangular lattice, a pair vortex lattice, stripes, and voids, which is consistent with a dominance of short-range two-scale repulsive interactions.

To better understand the structure of these phases, let us examine the RDF for each phase, which are shown in Fig. 5 (note that the ordering of the panels matches the ordering of Fig. 4). For the ring phase of Fig. 4(a), $g(r)$ has three pronounced peaks indicating the nearest-neighbor distance, next-nearest-neighbor distance, *etc.* inside the ring. In between the peaks, $g(r)$ remains finite because the vortices do not form an even lattice inside the ring. For the clustered ring phase [see Fig. 4(b)], the first peak is very pronounced and narrow, indicative of the particles in each cluster being roughly equidistant. The second peak characterizes nearest-neighbor distance between clusters, and the subsequent peaks the distance between next-nearest-neighbor clusters, *etc.* The long distances between the peaks indicate that the clusters are

small compared to their separation.

The modulated supercluster of Fig. 4(c) likewise has a sharp, narrow peak in $g(r)$ representing the nearly equidistant particle separation inside each cluster. For the stripe/void-rich phase [see Fig. 4(d)], we observe several prominent peaks in $g(r)$ that are largely consistent with the RDF for a triangular lattice, with broadening of the peaks due to the mixing of phases.

The superclusters shown in Fig. 4(e) possess short range periodicity inside each cluster, resulting in two narrow peaks in $g(r)$ which are so close together that the second peak appears as a shoulder. The successive peaks illustrate the distance between clusters and are broadened because of the finite size of each cluster. Because the clusters are widely separated, there are additional broad peaks in $g(r)$ that occur for large r and describe the supercluster separation. The RDF of the concentric ring phase [pictured in Fig. 4(f)] is remarkably similar to the $g(r)$ for the supercluster phase [Fig. 4(e)]. Unlike the supercluster phase, $g(r)$ remains finite for r smaller than the diameter of the outer ring due to the particles spreading out evenly throughout each ring.

Finally, we discuss the radial distribution functions of more conventionally ordered phases. The lattice phase [see Fig. 5(g)] possesses much more long-range order than all other phases considered, with peaks at $r = a, \sqrt{3}a, 2a, \sqrt{7}a, 3a, \dots$, where a is the nearest-neighbor distance for a triangular lattice. The dimer lattice phase [see Fig. 5(h)] has a clearly defined peak describing the dimer separation. Because the pairs prefer to line up end-to-end, the peaks that would describe the triangular lattice are broadened significantly and the long-range order cannot be observed in $g(r)$. The stripe phase [see Fig. 5(i)] has several regularly spaced peaks coinciding perfectly with the separation of particles along each stripe. Here, broadening occurs due to both bending of the stripes and the presence of other stripes. The void phase [see Fig. 5(j)] only has short-range periodicity, as evidenced by the pronounced features for small r .

In this paper, we studied vortex states in general layered superconductor-insulator-superconducting structures, made of different superconducting layers. The vortices are subject to interactions with multiple length scales. We have shown that these layered systems have an unusual magnetic response: vortex supercluster structures, which can consist of clusters of clusters, rings, clusters in a ring, or have coexistence of stripes, voids, and lattice phases. This can provide an experimental tool to deduce information about vortex interactions from observation of their ordering in real experiments. Besides that it indicates that one can use layered superconducting structures for the realization and study of rich and unique pattern forming systems. In further studies we plan to address effect of disorder and pinning on these vortex states, as well as their manifestations in the transport properties of layered structures.

We thank M. Touminen and C. Santangelo for discussions. This work was supported by NSF Award No. DMR-0955902 (C.N.V., Q.W. and E.B.) by Knut and Alice Wallenberg Foundation through the Royal Swedish Academy of Sciences (E.B.), Swedish Research Council (E.B. AND K.S.). The computations were partially performed on resources provided by the Swedish National Infrastructure for Computing (SNIC) at National Supercomputer Center at Linköping, Sweden.

-
- [1] C. J. Olson Reichhardt, C. Reichhardt, and A. R. Bishop, *Phys. Rev. E* **82**, 041502 (2010)
 - [2] C. J. Olson Reichhardt, C. Reichhardt, and A. R. Bishop, *Phys. Rev. E* **83**, 041501 (Apr 2011)
 - [3] E. Smørgrav, J. Smiseth, E. Babaev, and A. Sudbø, *Phys. Rev. Lett.* **94**, 096401 (2005)
 - [4] S. A. Parameswaran, S. A. Kivelson, E. H. Rezayi, S. H. Simon, S. L. Sondhi, and B. Z. Spivak, *Phys. Rev. B* **85**, 241307 (2012)
 - [5] D. G. Ravenhall, C. J. Pethick, and J. R. Wilson, *Phys. Rev. Lett.* **50**, 2066 (1983)
 - [6] G. Malescio and G. Pellicane, *Nature Materials* **2**, 97 (2003)
 - [7] M. A. Glaser, G. M. Grason, R. D. Kamien, A. Komrlj, C. D. Santangelo, and P. Ziherl, *Europhys. Lett.* **78**, 46004 (2007)
 - [8] A. A. Abrikosov, *Sov. Phys. JETP* **5**, 1174 (1957)
 - [9] G. Blatter, M. V. Feigel'man, V. B. Geshkenbein, A. I. Larkin, and V. M. Vinokur, *Rev. Mod. Phys.* **66**, 1125 (1994)
 - [10] E. Babaev and M. Speight, *Phys. Rev. B* **72**, 180502 (2005)
 - [11] V. Moshchalkov, M. Menghini, T. Nishio, Q. H. Chen, A. V. Silhanek, V. H. Dao, L. F. Chibotaru, N. D. Zhigadlo, and J. Karpinski, *Phys. Rev. Lett.* **102**, 117001 (2009)
 - [12] T. Nishio, V. H. Dao, Q. Chen, L. F. Chibotaru, K. Kadowaki, and V. V. Moshchalkov, *Phys. Rev. B* **81**, 020506 (2010)
 - [13] V. O. Dolocan, C. Veauvy, F. Servant, P. Lejay, K. Hasselbach, Y. Liu, and D. Mailly, *Phys. Rev. Lett.* **95**, 097004 (2005)
 - [14] P. G. Björnsson, Y. Maeno, M. E. Huber, and K. A. Moler, *Phys. Rev. B* **72**, 012504 (2005)
 - [15] R. Prozorov, A. F. Fidler, J. R. Hoberg, and P. C. Canfield, *Nature Phys.* **4**, 327 (2008)
 - [16] R. Geurts, M. V. Milošević, and F. M. Peeters, *Phys. Rev. B* **81**, 214514 (2010)
 - [17] J. Carlström, E. Babaev, and M. Speight, *Phys. Rev. B* **83**, 174509 (2011)
 - [18] J. Carlström, J. Garaud, and E. Babaev, *Phys. Rev. B* **84**, 134515 (2011)
 - [19] S.-Z. Lin and X. Hu, *Phys. Rev. B* **84**, 214505 (2011)
 - [20] M. Silaev and E. Babaev, *Phys. Rev. B* **84**, 094515 (2011)
 - [21] M. Silaev and E. Babaev, *Phys. Rev. B* **85**, 134514 (Apr 2012)
 - [22] V. H. Dao, L. F. Chibotaru, T. Nishio, and V. V. Moshchalkov, *Phys. Rev. B* **83**, 020503 (2011)
 - [23] J. Garaud, D. F. Agterberg, and E. Babaev, *Phys. Rev. B* **86**, 060513 (2012)
 - [24] J. A. Drocco, C. J. Olson Reichhardt, C. Reichhardt, and A. R. Bishop, arXiv:1207.5834
 - [25] J. Gutierrez, B. Raes, A. V. Silhanek, L. J. Li, N. D. Zhigadlo, J. Karpinski, J. Tempere, and V. V. Moshchalkov, *Phys. Rev. B* **85**, 094511 (2012)
 - [26] Y. H. Liu, L. Y. Chew, and M. Y. Yu, *Phys. Rev. E* **78**, 066405 (2008)
 - [27] V. M. Stojanović, W. Vincent Liu, and Y. B. Kim, *Annals of Physics* **323**, 989 (2008)
 - [28] M. G. Alford and G. Good, *Phys. Rev. B* **78**, 024510 (2008)
 - [29] E. Babaev, J. Carlström, J. Garaud, M. Silaev, and J. Speight, *Physica C* **479**, 2 (2012)
 - [30] J. Pearl, *Appl. Phys. Lett.* **5**, 65 (1964)
 - [31] G. Malescio and G. Pellicane, *Phys. Rev. E* **70**, 021202 (2004)
 - [32] P. J. Camp, *Phys. Rev. E* **68**, 061506 (2003)
 - [33] P. J. Camp, *Phys. Rev. E* **71**, 031507 (2005)
 - [34] See Supplemental Material <http://link.aps.org/supplemental/11.1103/PhysRevLett.XXX.XXXXXX> for a full description of the simulations and additional discussion of the potentials
 - [35] D. Landau and K. Binder, *A Guide to Monte Carlo Simulations in Statistical Physics* (Cambridge University Press, Cambridge, 2005)
 - [36] J.-P. Hansen and I. R. McDonald, *Theory of Simple Liquids* (Dover, New York, 1986)
 - [37] H. Fangohr, S. J. Cox, and P. A. J. de Groot, *Phys. Rev. B* **64**, 064505 (Jul 2001)
 - [38] Although long-range ordering of the superclusters and concentric rings is not present in the final MD configurations shown Figs. 4(e) and 4(f), simulations of $N_v = 1000$ and $N_v = 2000$ vortices exhibit similar long-lived metastable configurations which ultimately order in a lattice.